THE AMAZON RIVER BREEZE AND THE LOCAL BOUNDARY LAYER: I. OBSERVATIONS

AMAURI PEREIRA DE OLIVEIRA

Departamento de Meteorología, Instituto Astronômico e Geofísico, Universidade de São Paulo, Brazil

and

DAVID R. FITZJARRALD

Atmospheric Sciences Research Center, State University of New York, 12205, U.S.A.

(Received in final form 18 June, 1992)

Abstract. Observations of the diurnal evolution of the planetary boundary layer over the Amazon rain forest, made at sites close to the confluence of the Solimões and Negro rivers (approximately at 3° S, 60° W) near Manaus, Amazonas, Brazil, show the existence of a diurnal rotation of the wind near the surface and the frequent presence of low-level nocturnal wind maxima. These circulations are shown to be plausibly explained as elements of a river and land breeze circulation induced by the thermal contrast between the rivers and the adjacent forest.

1 Introduction

The Amazon Basin occupies approximately four million square kilometers, much of which is made up of large bodies of water associated with the Amazon river and its affluents (Dickinson, 1987). The climate of this region is characterized by a distinct dry season between July and December and a wet season between March and June, both related to the migration of the equatorial trough (Riehl, 1979). As a result, the meridional circulation in the region is dominated by horizontal convergence at low levels and divergence at high levels, while the zonal circulation is characterized by easterly winds at the lower levels and westerly flow at higher levels (Dickinson, 1987). Recently, Oliveira (1990) and Greco *et al.* (1992) have presented case studies in support of the hypothesis that local "river breeze" circulations may have an important influence on local climate and weather. It has been suspected for some time that circulations associated with the river can be important to the local weather. That the river is frequently observed to be cloud-free in satellite images (Molion and Dellarosa, 1990) is indirect evidence that subsidence, possibly associated with a river breeze circulation, occurs during the daytime over the rivers. Molion and Dellarosa have suggested that river-breeze convergence may depress rainfall along the river and enhance it inland. Since climate stations in Amazonia are concentrated near population centers along the river, such local influences on climate might bias climatological estimates of rainfall used to calibrate remote sensing techniques.

A limited number of observations of the low-latitude planetary boundary layer (PBL) are available. Observations obtained in Venezuela during VIMHEX

Boundary-Layer Meteorology **63**: 141–162, 1993.

(9.5° N, 67° W, described in Betts, 1976) indicated that the equatorial PBL structure is similar to that typical in higher latitude continental areas, with a daytime mixed layer, 1000–2000 m deep, limited above by a statically stable layer, with a nocturnal stable layer at the surface. The Amazon Boundary Layer Experiments, ABLE 2a (July–August of 1985) and ABLE 2b (April–May of 1987), conducted in the Brazilian portion of the Amazon Basin during the dry and wet seasons, respectively, provided the first comprehensive data set describing the Amazonian boundary layer. These experiments, part of a program to determine the intensity of sources and sinks of the atmospheric trace chemical substances, are described in detail elsewhere (Harriss *et al.*, 1988). The meteorological component of these experiments is described by Garstang *et al.* (1989). Results presented by Martin *et al.* (1988) indicate that the bulk characteristics of the boundary layer over the central Amazon (3° S, 60° W) are broadly similar to those reported by Betts in Venezuela.

These studies gave emphasis to thermodynamic structure. In this work we return to the data from ABLE-2 to investigate momentum transports, to describe the diurnal evolution of the thermodynamic and dynamic structure of the PBL over the equatorial portion of the Amazon Basin, and to identify the most important physical mechanisms responsible for the observed diurnal evolution of the boundary layer. Our approach, distinct from that of Greco *et al.* (1992), is to form composites using relatively large amounts of data to examine diurnal variability of the boundary layer. The task is to identify the relative contribution of three factors on diurnal PBL evolution: (a) the influence of seasonal differences in the large-scale flow; (b) effects of the thermal contrast induced by the great rivers (Amazonas, Negro and Solimões), and (c) vertical redistribution of momentum due to the diurnal evolution of the PBL. In this paper, we present primarily observational results, deferring comparison with model simulations to a companion paper. We aim to test the hypothesis that river breeze circulations have an important effect on the local boundary-layer climate.

2. Background

2.1. Observational sites

The position of surface stations and sonde launching sites at Ducke Reserve, Embrapa and Carapanã and the urban area of Manaus is shown in Figure 1. This region is dominated by the confluence of great rivers: the Amazonas (to the east), the Negro (to the northwest) and the Solimões (to the southwest). Note that the width of the rivers is comparable to the distance between adjacent stations and from the closest station to the water. (Distances in km are indicated in Figure 1 along the sides of the triangles joining the three stations.)

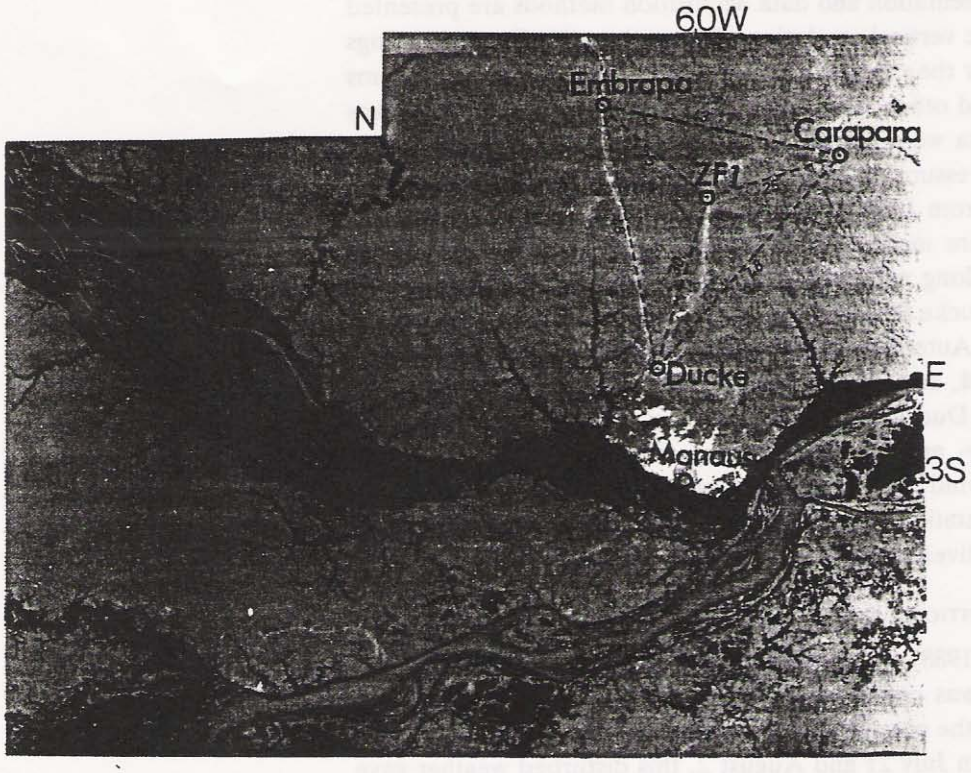

Fig. 1. Landsat image of the area of the ABLE 2 experiments. The Manaus urban area, the Amazonas, Negro and Solimões River are indicated. Stations are located at the vertices of a mesoscale triangle: Ducke Reserve, Embrapa, ZF-1, and Carapanã. Distances between stations (km) are shown along the dashed connecting lines.

2.2 Instrumentation

During ABLE 2a (1985, dry season), tethered balloon soundings were made 20 km north of Manaus at the Ducke Forest Reserve, while the rawinsondes were launched at the Ponte Pelada Military Airport in Manaus. During ABLE 2b (1987, wet season), tethered balloon and rawinsonde launches were made at the Ducke Forest Reserve, Embrapa and Carapanã. During the dry season experiment, 70 daytime (06–18 LST) rawinsonde soundings and 24 nighttime (18–06 LST) soundings are available. There were 337 tethered balloon soundings. During ABLE 2b, 363 soundings were made, distributed among the three sites: 94 soundings at Ducke, 97 at Embrapa and 94 at Carapanã. There are 24 nocturnal soundings at Ducke, 48 at Embrapa and 16 at Carapanã.

An A.I.R., Inc. Airsonde system was used in both campaigns. During 1985, the sondes were tracked by a RD-65 radio theodolite; in 1987 the RD-65 radio theodolite was placed at Embrapa and GMD radio theodolites were used at Ducke

Carapanã. Details of instrumentation and data acquisition methods are presented in Garstang *et al.* (1989). The vertical resolution of the tethered balloon soundings was typically 4 m and that for the rawinsonde data was 10–15 m. Due to problems with the pressure sensors and other errors, each of 395 soundings from 1987 was individually checked and data were removed for those levels that did not exhibit monotonically decreasing pressure with time. Each sounding was then linearly interpolated to a 5 mb grid from 1000 to 400 mb.

Surface measurements were made in 1985 by an automated weather station (Shuttleworth *et al.*, 1985) along with turbulence observations (Fitzjarrald *et al.*, 1988) at the 45 m tower at Ducke Reserve. During ABLE 2b there was a network of four PAM II (Portable Automated Mesonet II) stations located at Ducke Reserve, Embrapa, Carapanã, and ZF-1 (Figure 1) as well as the turbulence and surface measurements at the Ducke tower (Fitzjarrald *et al.*, 1990). Each PAM II station reports pressure, dry- and wet-bulb temperature, zonal and meridional components of horizontal wind and rainfall amount-at 1–min intervals. More details concerning instrumentation used in ABLE 2a and 2b can be found in Garstang *et al.* (1989) and Oliveira (1990).

2.3. Meteorological conditions

According to Harriss *et al.* (1988), the first period of the dry season experiment (July 15 through 20, 1985) was characterized by widespread disturbed weather over the Amazon Basin, and the precipitation records indicated that this condition prevailed at Manaus. Between July 21 and August 2, this disturbed weather gave way to a more tranquil regime as a subtropical anticyclone moved equatorward and centered over the Brazilian Northeast. From August 3 through 5, the disturbed weather observed in the first period gradually dominated the weather in the Manaus area. Greco *et al.* (1989) note that the wet season in 1987 was drier than the climatological normal at Manaus. Rainfall records indicate that the weather regime during ABLE 2b can be characterized by a highly disturbed period, between April 13 and May 3, when most of the precipitation was produced by convective systems formed in the coastal region of South America or within the Amazon Basin, and a less disturbed period between May 4 and 14, when locally occurring systems produced most of the precipitation. For ABLE 2b, we have adopted the convective classification proposed by Greco *et al.* (1988). Diurnally occurring systems refer to the synoptic conditions in which the convective activity (clouds) appear to have been produced locally, while basin and coastal occurring systems refer to the convective activity induced by systems originally from the Amazon Basin and coastal areas to the northeast of South America, respectively.

2.4. Mean vertical structure

To investigate seasonal differences in the vertical momentum transport in the PBL, one must characterize the environment in which the boundary layer grows. The mean profiles of potential temperature and mixing ratio (presented in Oliveira,

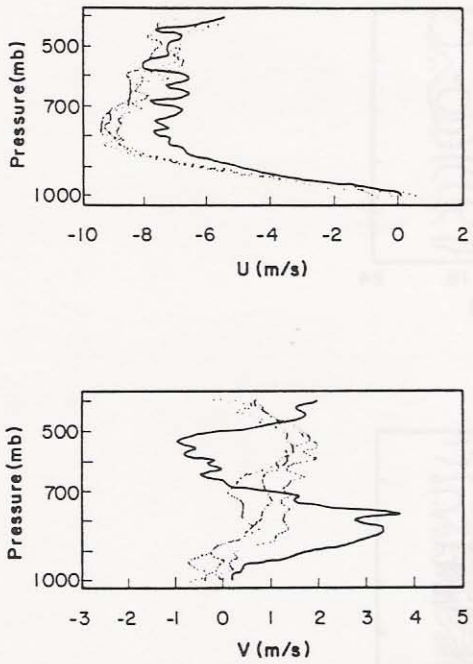

Fig. 2. Vertical profile of the averaged winds. Top: zonal component (m/s); Bottom: meridional component of the wind speed (m/s), for rawinsondes launched in Manaus between July 15 and August 5, 1985 (continuous line) and Ducke, Embrapa and Carapanã, between April 13 and May 13, 1987 (dotted lines).

1990) are comparable to those seen in other tropical areas, and these seasonal differences are not likely to affect the thermodynamic evolution of the equatorial PBL. Since any local river breeze circulations will be forced along a line normal to the river, seasonal changes in mean wind direction and wind shear intensity would be expected to lead to different effects on these winds. The most marked seasonal variation is in the mean wind direction in the dry and wet periods (Figure 2). The zonal flow was easterly (negative) and evenly distributed (approximately 7 m/s) throughout the first 600 mb in the dry season; during the wet season the zonal flow presented a relative maximum of 9–10 m/s around 800 mb. The mean meridional component (Figure 2) in the dry season was southerly with a relative maximum of 3 m/s around 800 mb; during the wet season it was still southerly but exhibited a relative maximum of 1.5–2.0 m/s near 500 mb, similar to that presented by Palmén and Newton (1969). The mean wind profiles simply indicate that during the dry season (July–August) the average Intertropical Convergence Zone (ITCZ) was located northward of the region so that the meridional flow is a maximum. During the wet season (April–May) the ITCZ was over the region and the meridional flow was no longer large.

Temperature, mixing ratio, and zonal and meridional wind speed components

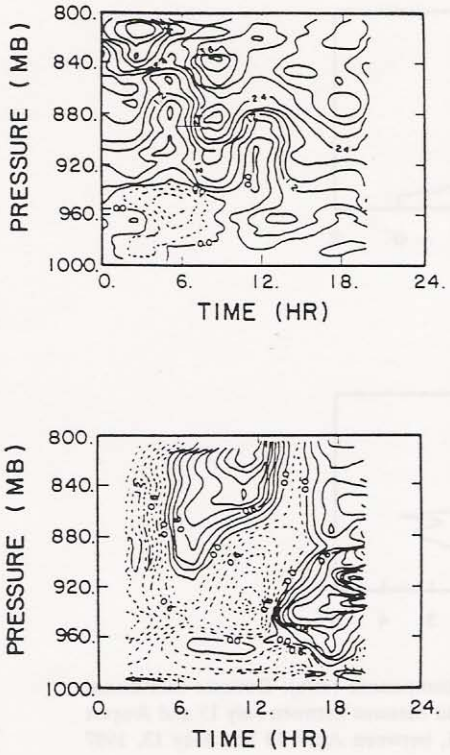

Fig. 3. Rawinsonde data between 1000 and 800 mb levels. Diurnal evolution of the mean vertical profile of the meridional component of the wind (m/s). Top: Manaus in 1985 (dry season); Bottom: Ducke Reserve in 1987 (wet season).

were evaluated for the experimental periods during 1985 and 1987 using both rawinsonde and tethersonde data. Time-height sections (Figure 3) were obtained by interpolating the hourly averaged soundings onto a two-dimensional grid. On average, the diurnal evolution of the first 200 mb of the atmosphere at Ducke in the wet season in 1987 is similar to that observed at Manaus in the dry season in 1985. In spite of the presence of higher frequency and intensity of cumulus convection, the PBL during the wet season in 1987 presents, on average, a stable layer during the night and a mixed layer during the daytime. The mean boundary-layer wind was easterly in the lowest 200 mb during the dry season in 1985 at Manaus, more intense during the night than during the day. A similar average diurnal evolution was observed at Ducke Reserve using tethersonde data in 1985. The average zonal component observed during the wet season in 1987 at Ducke Reserve was similar to that observed during the dry season in 1985 at Manaus. The predominant wind direction was easterly during both seasons, in accord with previous climatological studies of the 850 mb winds (Molion, 1987, pp. 392, 394). The averaged zonal wind components observed in Embrapa and Carapanã in the

wet season of 1987 (not shown) are similar to ones observed at Ducke Reserve. The diurnal pattern presented by the mean winds and thermodynamic quantities in the lowest 200 mb in both seasons reflect the expected diurnal difference in coupling between the surface and the air aloft. In the first 100 mb, easterly flow is more intense during the night and less intense during the day, especially during the afternoon. During the day, the turbulent vertical mixing is intensified by the presence of thermals, the stress increases, and the flow is decelerated.

We were surprised by the similarity in boundary-layer observations between the dry and the wet seasons, since it was expected that cumulus convective outflows would disturb the PBL sufficiently during the wet season to make distinct features vanish in longer-term averages. The most striking feature is the diurnal evolution of the average meridional component of the wind observed in both seasons. During the dry season in 1985 at Manaus and the wet season in 1987 at the Ducke Reserve (Figure 3), the meridional component was negative during the night and morning and shifted to positive during the afternoon. Since the mean flow has a meridional component from the south (Figure 2), northerly flow during the night and morning opposes the mean southerly flow. Similar diurnal patterns (not shown) were identified at Embrapa and Carapanã in the wet season, and at Ducke Reserve and in the dry season.

Though the situation is somewhat complicated by the fact that only the Amazon river is aligned approximately E-W and the Negro river is aligned NW-SE (Figure 1), the negative meridional wind component is largely from the forest toward the rivers and the positive meridional component indicates a flow toward the forest. The flow from the forest toward the rivers is observed in a much deeper layer (100–120 mb) in the wet season (1987) than the 60–80 mb thick layer observed in the dry season (1985). In the dry season, the onset of the "river breeze" ($V > 0$) occurs earlier at the city of Manaus than at the Ducke Forest Reserve, 20 km inland. During the wet season, the onset of $V > 0$ occurs later and is weaker for sites located farthest from the river.

In summary, the hourly average fields analyzed above indicate the existence of a circulation at low levels of the atmosphere over the region of the ABLE 2a experiment (dry season 1985) that is also present during the ABLE 2b experiment (wet season 1987). The observed circulation has a diurnal cycle with northeasterly flow (toward the river) during the night and morning and southeasterly flow (away from the river) during the afternoon and evening. This pattern is consistent with the hypothesis of a "river breeze" circulation produced by the thermal contrast between the rivers (Amazon and Negro) and the forest. The seasonal differences are plausibly related to larger daytime river-land temperature contrasts that occurred during the less cloudy dry season.

2.5. Aircraft data

Unique observations of the river breeze were made with the NASA Electra research aircraft during the ABLE 2 experiments. A complete description of the

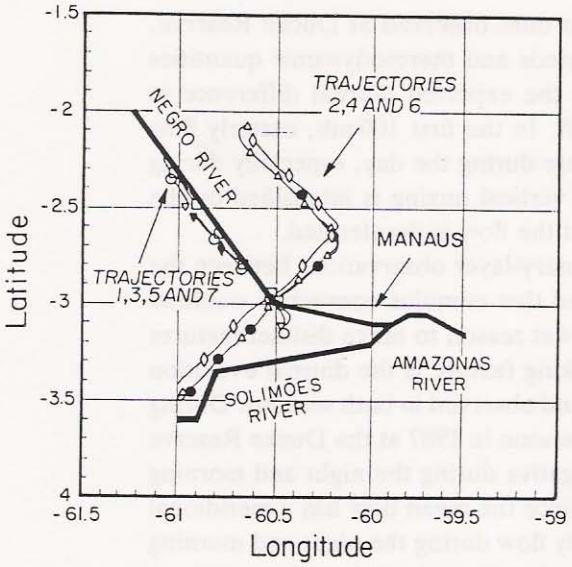

Fig. 4. Schematic map of the experimental area and the trajectories of flights 10 (12–18 LT) and 11 (03–10 LT) made on July 29 and 31, 1985. The trajectories are indicated by numbers 1–7. The airplane flew from south to north during the parallel trajectories (1, 3, 5 and 7), and from north to south during the perpendicular trajectories (2, 4 and 6).

airplane measurements can be found in Harriss *et al.* (1988). Aircraft measurements made near the river (Figure 4) included wind speed, wind direction, air temperature, dew point temperature and surface radiation temperature. The presence of a thermal contrast between the river and the forest and associated local winds are clearly indicated (Figures 5 and 6). Flights 10 and 11, flown at or below 250 m altitude on July 29 and 31, 1985, were designed specifically to study the forest-river interface (Figure 4). Flight 10 (1200–1800 LT) results are typical of daytime conditions, while flight 11 (0300–0930 LT) represents primarily the nocturnal situation. The wind pattern observed during the late morning trajectories 4 and 6 conforms to the hypothesis of a river breeze circulation, inducing a positive cross-river wind component to the north of the Negro River and a negative cross-river wind component to the south. We hypothesize that the circulations around the river area were asymmetric because of the easterly mean wind. Based on Figure 5, it appears that the horizontal extent of the river breeze is approximately 25 km.

2.6. Surface data

The rawinsonde and tethered balloon observations indicate the presence of a distinct circulation below 500 m in both seasons, with flow from the forest toward the river during the night and early morning, with a tendency to flow from the

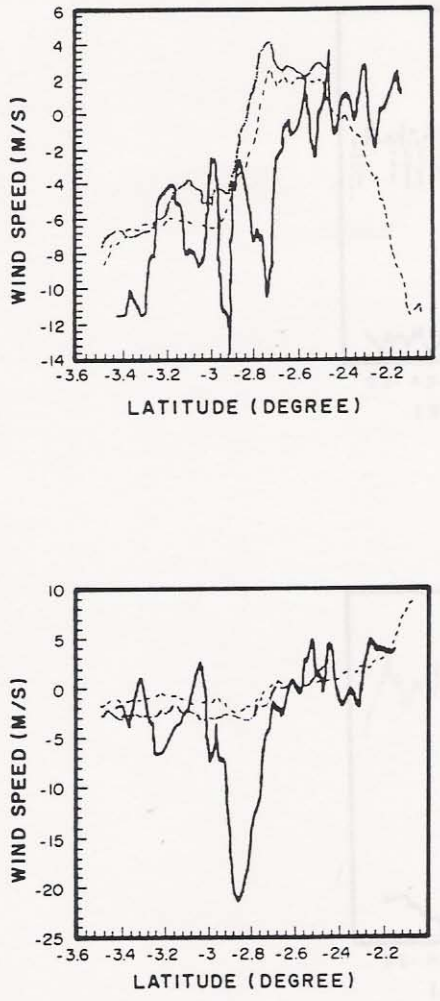

Fig. 5. Cross-river (top) and river-parallel river (bottom) wind components observed by the aircraft during the dry season in 1985. The dashed line corresponds to the trajectory 4, flight 10, 1215–1245LT, on July 29. The dotted (or thin continuous) line corresponds to trajectory 6, flight 10, 1450–1520LT, on July 29. The thick continuous line corresponds to the trajectory 2, flight 11, 0630–0645LT, July 31.

river toward the forest in the afternoon and evening (see Section 2.4). Here we examine the more detailed temporal record of the diurnal change available in the surface data to identify the presence of a diurnal cycle in the wind, horizontal pressure gradient, horizontal temperature gradient, and the divergence of horizontal wind.

We identified the diurnal cycle and horizontal pressure and temperature gradients using observations made by the four PAM stations (Figure 1). Data were split into two periods according to the Greco *et al.* (1989) classification: (1) Julian

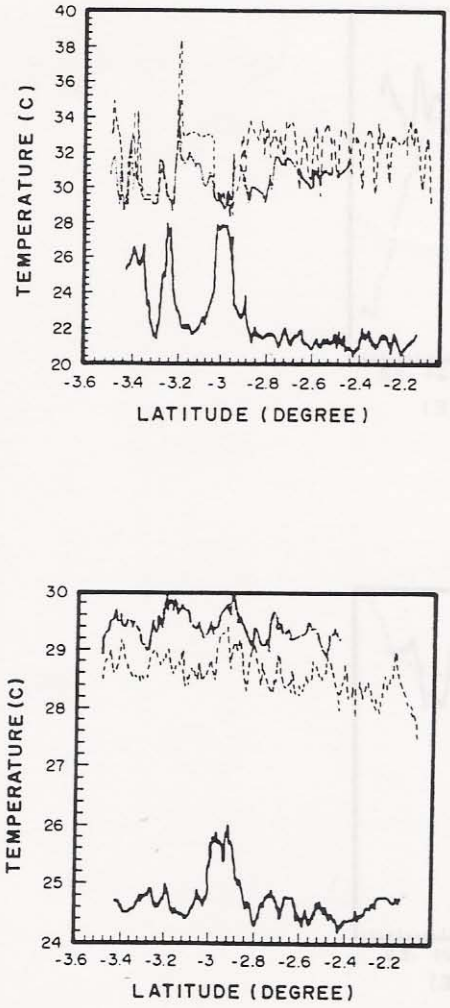

Fig. 6. Surface temperature (top) and air temperature (bottom). The dashed line corresponds to the trajectory 4, flight 10, 1215–1245LT, on July 29, 1985. The dotted (or thin continuous) line corresponds to trajectory 6, flight 10, 1450–1520LT, on July 29. The thick continuous line corresponds to the trajectory 2, flight 11, 0630–0645LT, July 31.

days 103–118 (April 13 through April 28, 1987), a relatively disturbed period; and (2) Julian days 118–133 (April 28 through May 13), a period with less convective disturbance. To reduce systematic instrumentation and siting errors, perturbation time series of temperature, humidity, and wind components were obtained by removing the station mean for each period. Since obstructions in the vicinity of the wind sensors can also lead to systematic high or low divergences, wind speeds were corrected using the direction-dependent transmission factor described by

Fujita and Wakimoto (1982). Scalar gradients and the horizontal wind divergence were then found using least-squares plane fits to the data at each station. Hourly-averaged horizontal gradients of pressure and temperature (Figure 7) demonstrate the existence of the diurnal cycle in the horizontal pressure gradient, with an area of high pressure over the southwestern vertex of the triangle between 1300 and 1700 LT, with a maximum of 0.5 mb/100 km at approximately 1300 LT. Though the magnitude of the pressure gradient decreases during the night period, it appears that there is relatively higher pressure northeast of the triangle between 2200 and 0300 LT with an amplitude of 0.1–0.2 mb/l00 km. Consistent with this result, the horizontal temperature gradient in Figure 7b also indicates the presence of a relatively warm area at the northeasterly vertex of the triangle during the day, with a maximum amplitude equal to 2 K/100 km. During the night, the warm area moves gradually to the south. The apparently anomalous temperature and pressure gradients at 1700 LT are perhaps the effects of the systematic late afternoon rainfall in the area (Greco *et al.*, 1989). The time series of pressure and temperature gradients are consistent with the hypothesis of a circulation induced by thermal contrast between the rivers and the adjacent forest. During all times of the day the pressure ard temperature gradients are out of phase.

We investigated the possibility that the correlation between temperature and pressure gradients resulted from temperature dependency of the pressure sensor. According to Brock *et al.* (1986), the residual instrumental error tendency for the pressure as a function of temperature for the range of temperature for which the observations were made are about one order of magnitude smaller than that shown by the observations. Details of this comparison are presented in Oliveira (1990). We believe that the surface temperature and pressure gradients may reasonably be considered to be valid. Diurnal changes in the surface divergence are not as pronounced in the hourly averaged data as are the temperature and pressure gradients. However, they are clearly identifiable on days when convective activity was less intense. We extracted the diurnally varying component of the temperature and pressure gradients and the divergence at the surface using a seasonal adjustment technique, SABL (Cleveland *et al.*, 1982). The resulting composition is less sensitive to temporal irregularities due to the convective activity than conventional harmonic analysis (Oliveira, 1990). During the first week of the second period (117–124 JD) the diurnally oscillating part of the divergence was most evident, exhibiting an amplitude of $2 \times 10^{-5}\,s^{-1}$, going from convergence to divergence approximately 1500–1600 LT, not greatly different from what one might expect from a symmetrical river breeze (1800 LT).

Polar plots of the average horizontal wind deviation from the diurnal mean at Ducke Reserve during the dry season in 1985 and at the PAM stations during the wet season in 1987 (Figure 8) show that hourly-averaged surface winds describe an elliptical trajectory that rotates clockwise with time. This feature is present at all surface stations, in both seasons (Oliveira, 1990). During the wet season, the

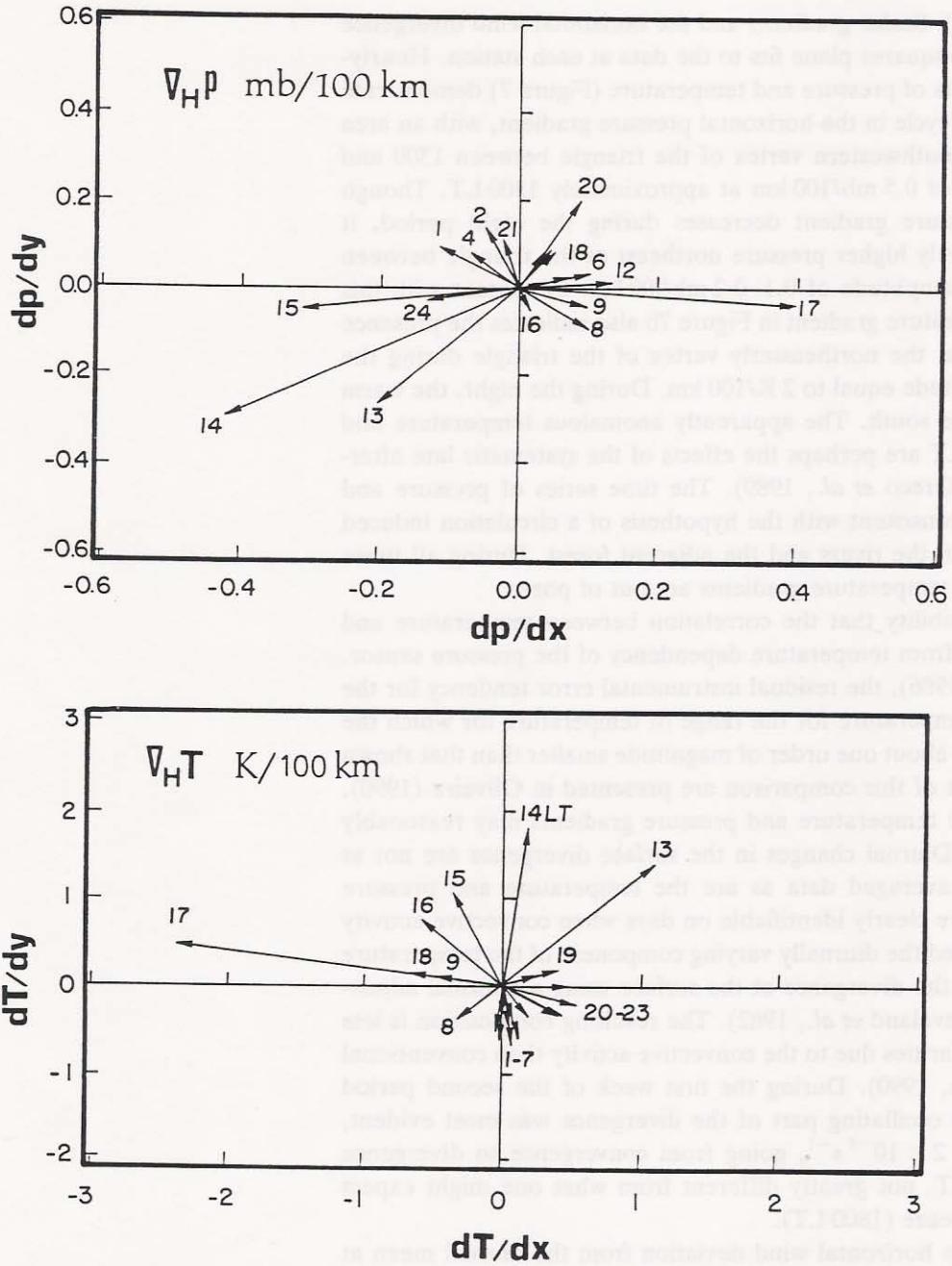

Fig. 7. Hourly-averaged horizontal (a) pressure gradient (mb/100 km) and (b) temperature gradient (K/100 km) for the second period of the ABLE 2b. Local time is indicated at each arrow.

rotation is better defined during the less disturbed second period. The major axis of the ellipse in the dry season of 1985 is parallel to the N–S direction, while during the less disturbed period of the wet season of 1987, the major axes are oriented in the NW–SW direction. The existence of elliptical trajectories on a polar plot in coastal areas in middle latitudes has been used as an indication of the presence of a thermal circulation associated with the sea breeze in the presence of Coriolis-forced rotation (Kusuda and Alpert, 1983). We hypothesize that these similar elliptical plots at the equator result from the effect of the entrainment of momentum associated with the growing PBL in the morning combined with an afternoon river breeze. It appears that the seasonal difference in major axis orientation is due to the seasonal difference in mean boundary-layer wind.

Preliminary to more detailed model studies, we constructed a horizontal momentum balance by integrating vertically throughout the PBL the equation of horizontal motion. We assume that: (a) the large-scale flow (indicated by U_0, V_0, W_0,) is in steady state and the horizontal advection of momentum is in balance with the horizontal pressure gradient ($\nabla_h p_0$); (b) the local circulation is confined vertically within the PBL (Pielke, 1984); (c) the local wind (the hourly averaged wind, V_m) is equal to the mean wind ($\langle V_m \rangle$) plus the thermal circulation wind ($V_m - \langle V_m \rangle$). The polar plots in Figure 8 correspond to the thermal circulation ($V_m - V_m\rangle$). (d) Accelerations that act on the entire mixed layer are reflected at the surface. Considering the assumptions above, the equation of motion of layer-averaged horizontal momentum can be written as:

$$\underset{(1)}{\partial V_m/\partial t} = \underset{(2)}{A_d} - \underset{(3)}{(1/\rho_m)\nabla_h p_m} + \underset{(4)}{(1/h)(\partial h/\partial t - w_h)(V_0 - V_m)} - \underset{(5)}{(1/h)(C_d|V_m|)\,V_m}$$

where V_m is the layer-averaged horizontal wind integrated through the PBL, $\langle V_m \rangle$ is the value of V_m averaged over one day, V_o is the free-atmosphere horizontal wind, w_h is the vertical wind speed at the top of the PBL, h is the height of the PBL, $\nabla_h p_m$ is the local horizontal pressure gradient, C_d is the drag coefficient and A_d is the layer-averaged horizontal advection of horizontal wind. Term (1) is the local rate of change of local wind; (2) is the horizontal advection of local wind produced by the large-scale flow; (3) is the local horizontal pressure gradient force; (4) is the turbulent entrainment of the local wind at the top of the PBL; (5) is the vertical advection of local wind produced by the large-scale flow; and (6) is friction at the bottom of the PBL.

Estimates of the daytime evolution of each term in the layer-averaged momentum equation are shown in Figures 9 and 10. To make these figures, we assumed: (1) the PBL height was constant at 250 m during the night and 1200 m during the day, values similar to those observed in Martin *et al.* (1988); (2) the drag coefficient varied from 0.010 during the nighttime to 0.125 during the daytime as reported by Fitzjarrald *et al.* (1988). Note that the local acceleration (term 1) is in phase with the horizontal pressure gradient force (term 3).

In Figure 9, negative values of acceleration parallel to the river are due to the

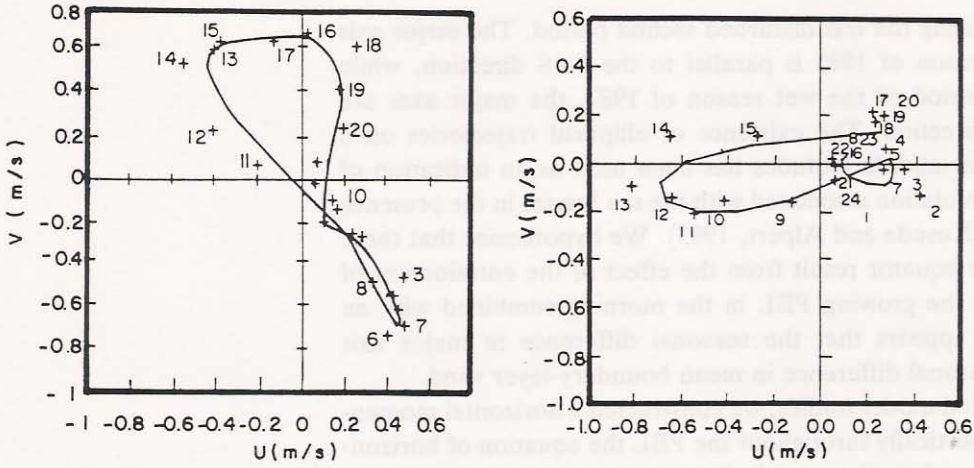

Fig. 8. Hourly-averaged surface wind deviation from the diurnal mean at Ducke Reserve; Left: Ducke Reserve during the entire dry season experiment 1985 (July 15 to August 5, 1985). Right: PAM II data obtained during the second period of the wet season experiment (April 28 to May 13, 1987). Numbers correspond to Local Time. Points are the actual values and the lines are the smoothed curves through these points.

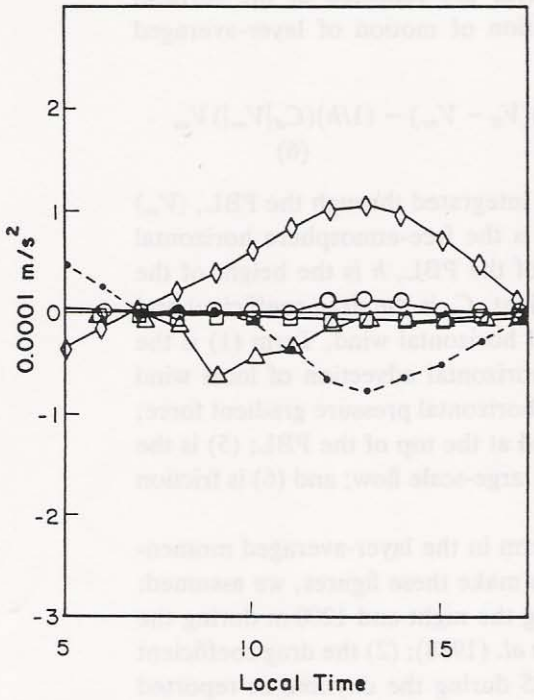

Fig. 9. Components of equation of motion normal to the river (N-S direction): Local rate of change (term 1, circles), horizontal pressure gradient acceleration (term 3, diamonds), entrainment (term 4, triangles), subsidence, surface friction (term 6, squares), and the unexplained residual (dash-dot).

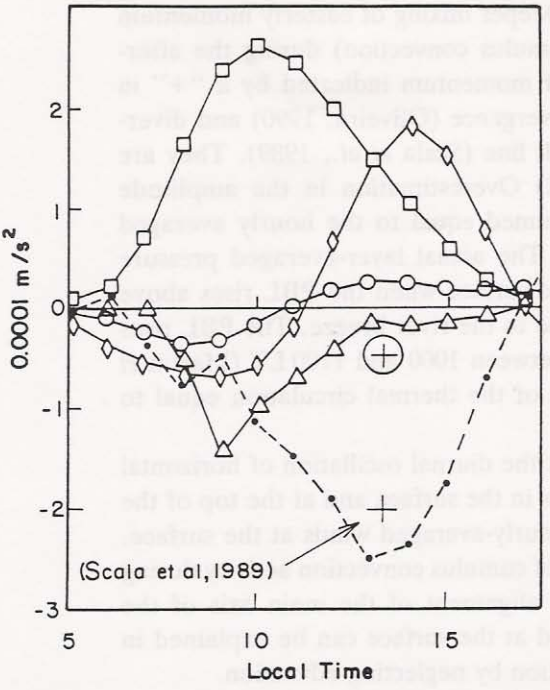

Fig. 10. Components of equation of motion parallel to the river (E-W direction): symbols are the same as in figure 9. Subsidence based on network-averaged horizontal divergence (term 5, cross in circle) and that estimated by Scala *et al.* (1989, cross) are also indicated.

turbulent flux of horizontal momentum at the top of the PBL (term 4) and positive values are due to the friction at the surface (term 6). The entrainment of momentum at the top of the PBL and the removal of momentum by friction at the surface reach a minimum and maximum respectively at 1000 LT, when the vertical evolution of PBL and the total wind at the surface reach a maximum. Because the total wind within the PBL is always negative in the x direction, the surface is always removing negative momentum, and the free atmosphere resupplies it since the easterly winds in the free atmosphere are larger than in the PBL. Perpendicular to the river (Figure 10), the local rate of change of wind is much smaller than the horizontal pressure gradient force, though the two terms are in phase between 10 and 15 LT. The entrainment of negative meridional momentum during the morning is related to the vertical evolution of the PBL, and is comparable to the horizontal pressure gradient. The over-all effect of friction on the momentum budget in the y direction is very small. The residual acceleration, corresponding to advection of horizontal momentum and the sum of any errors, is largest between 11 and 15 LT. This residual acceleration cannot be attributed to horizontal advection, since direct estimates using the network observations indicate values that are one order of magnitude smaller. Therefore, we suggest

that the residual acceleration is due to: (1) Deeper mixing of easterly momentum due to the enhanced convective activity (cumulus convection) during the afternoon. Estimates of the vertical advection of momentum indicated by a "+" in Figure 10 were based on hourly-averaged divergence (Oliveira, 1990) and divergence associated with the passage of a squall line (Scala *et al.*, 1989). They are comparable to the residual acceleration; (2) Overestimation in the amplitude of the layer-averaged pressure gradient, assumed equal to the hourly averaged horizontal pressure gradient at the surface. The actual layer-averaged pressure gradient will be a fraction of that seen at the surface when the PBL rises above the vertical extent of the thermal contrast due to the river breeze. The PBL rises above the depth of the thermal circulation between 1000 and 1100 LT (Martin *et al.*, 1988) corresponding to a vertical extent of the thermal circulation equal to 500–600 m.

The data analysis above suggests to us that the diurnal oscillation of horizontal pressure gradient and the turbulent exchanges in the surface and at the top of the PBL explains the diurnal oscillation of the hourly-averaged winds at the surface. The discrepancies may be explained in terms of cumulus convection activity during the afternoon. The elliptical shape and the alignment of the main axis of the forcing (pressure gradient) and the local wind at the surface can be explained in terms of the layer-integrated equation of motion by neglecting advection.

In the absence of turbulence, the bulk momentum equation indicates that for a horizontal pressure gradient oscillating diurnally, the forcing (pressure gradient force) and the local acceleration would be in phase, and the local wind would lag by 90°. Thus, the main axis of the local wind ellipse would be 90° out of phase with the main axis of the horizontal pressure gradient force. However, Figures 9 and 10 illustrate that there is no phase angle between the main axis of the wind and the horizontal pressure gradient ellipses. If a linear surface friction were introduced, it is easy to show that the phase angle between the wind and the forcing (pressure gradient force) would decrease, and the local rate of change of the wind would be out of phase with the forcing in the forward sense. Therefore, one would expect that the local wind would catch up with the horizontal pressure gradient force during the day time and stay behind during the night time. In this case, the local rate of change of the local wind would pass the horizontal pressure gradient during the daytime and stay with it during the night. Thus, the increase in friction and entrainment of momentum during the daytime causes the main axis of the local wind ellipse to align with the main axis of horizontal pressure gradient ellipse.

3. Low Level Maximum Winds

Analysis of the vertical profiles of horizontal wind speed and direction measured with the tethered balloon in 1985 at Ducke Reserve and during 1987 at Ducke Reserve, Embrapa and Carapanã indicated the presence of a low-level maximum

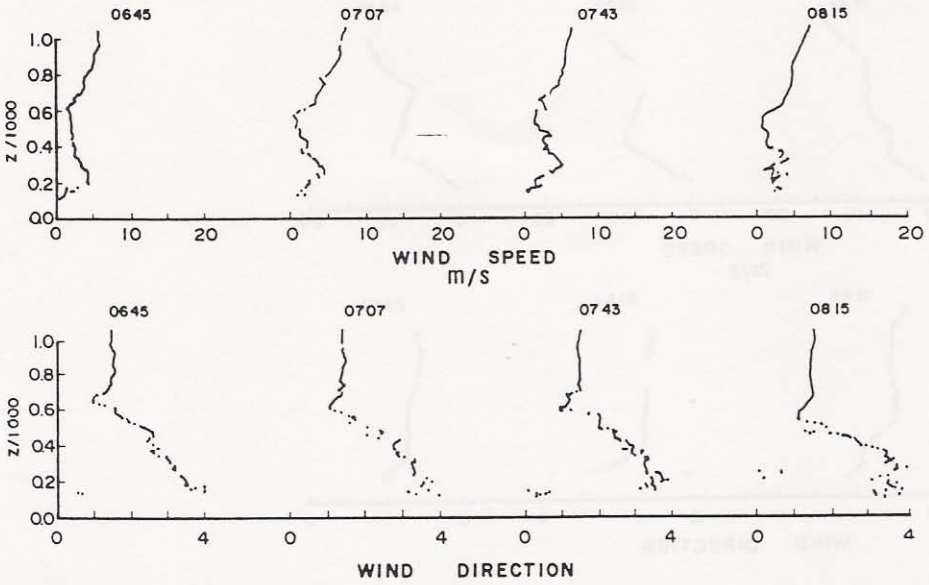

Fig. 11. Example of the first class of low level wind speed maxima (J1) observed on July 23, 1985 at Ducke Reserve. Vertical profiles of wind speed (top) and wind direction (bottom) are shown for the designated local times.

wind speed (LLM) during periods when the surface layer was statically stable, when there was appreciable radiational cooling (surface net radiation < -30 W/m^2, Oliveira, 1990, p 105). The presence of nocturnal wind maxima in the boundary layer has frequently been associated with the Coriolis effect at middle latitudes (Whitman, 1976), but no such explanation is relevant here. Greco *et al.* (1992) presented several case studies of this phenomenon based on ABLE-2 data. We have analyzed a much larger number of cases of these boundary-layer wind maxima. Details of the objective classification of low-level wind maxima are presented in Oliveira (1990). Based on the vertical profile of wind direction, the LLM can be divided into two distinct classes, defined by the presence (class J1) or absence (class J2) of appreciable vertical directional wind shear. An example of LLM of the first class (J1) observed on the morning of July 23, 1985 at the Ducke Reserve (Figure 11) illustrates the presence of a local wind speed maximum of 5 m/s at 100 m embedded in a deeper layer 500 m thick, in which the wind direction shifted gradually from northerly (at the surface) to easterly (at 600 m). This LLM remained stable from 6:45 to 8:15 LT, when thermal convection began to destroy it. An example of LLM of the second class J2 (Figure 12) illustrates a LLM present at 500 m in the morning and 300 m in the evening. The LLM is strong in the morning soundings, approximately 18 m/s, but less so in the evening, approximately 10 m/s.

Both types of LLM were also observed in the 1987 experiment. These LLM

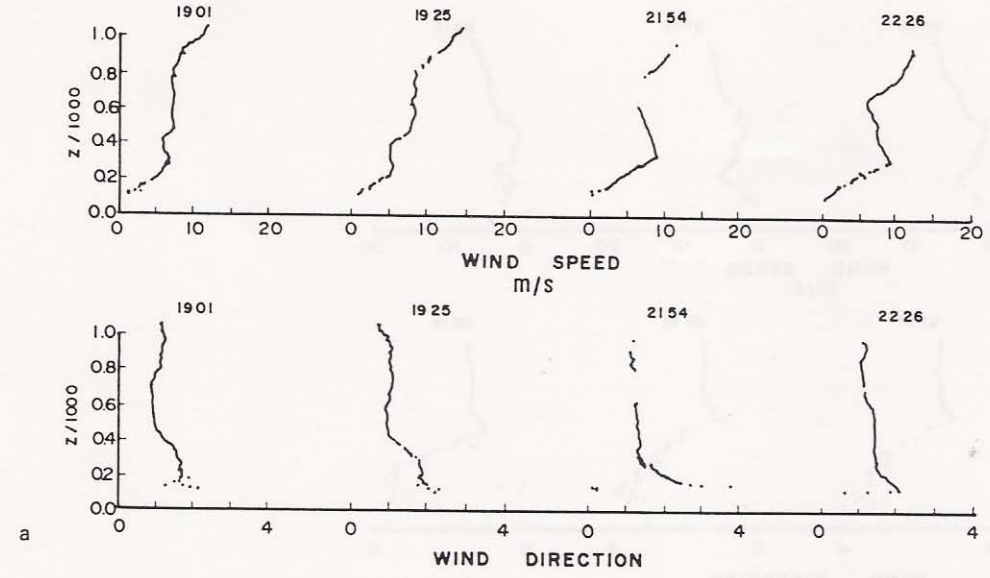

a

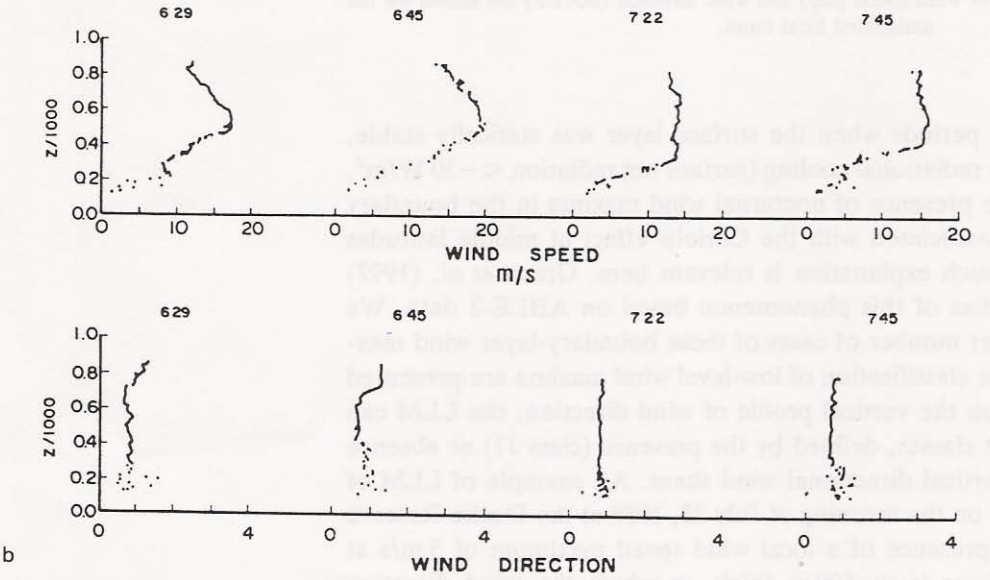

b

Fig. 12. (a) Example of the second class of low level wind speed maxima (J2) observed on July 25, 1985 at Ducke Reserve. Vertical profiles of wind speed (top) and wind direction (bottom) are shown for the designated local times. (b) A second example of the second class of low level wind speed maxima (J2) observed on July 25, 1985 at Ducke Reserve. Vertical profiles of wind speed (top) and wind direction (bottom) are shown for the designated local times. Wind direction is divided by 90°.

occurred with high frequency in both seasons, 12 out of 16 days in 1985 and 18 out of 29 days in 1987, at Ducke Reserve. The number of J1 cases was much larger in 1985 than in 1987, 6 out 12 days in 1985 and 6 out of 18 days in 1987. The J1 case occurred predominantly in early morning (06–10 LT), while J2 cases were observed at various times during the night. The J1 cases occurred during the period when weather conditions were disturbed, while J2 occurred when the weather conditions were undisturbed in 1985 (see Section 2). In 1987, J1 cases occurred more often at all three sites when the region was under the influence of the coastal systems (defined using the Greco *et al.*, 1989, classification) On the other hand, the J2 cases occurred more often when the region was under the influence of local and basin occurring systems. Because it is confined to low levels (200–400 m) and is characterized by northerly winds, we hypothesize that the J1 wind maxima are manifestations of the river breeze circulation. The J2 maxima, however, are deeper (up to 1000 m) and may be associated with a larger scale regional pressure gradient, perhaps associated with the disturbance lines reported by Greco *et al.* The distinction between the two types of wind maxima will probably only be clarified when simultaneous mesoscale pressure gradient and vertical sounding data become available.

4. Conclusions and Comments

We have identified several distinctive features of the boundary-layer structure and its dynamics in the central Amazon: (1) Despite the high frequency and intensity of cumulus convection activity, it is possible to identify typical characteristics of CBL development in the average diurnal thermodynamic, moisture and dynamic fields during the wet season in 1987 at four sounding stations near the river. Even though the amplitude of the diurnal cycle of average potential temperature and mixing ratio is larger during the dry season, there are no significant differences in the average diurnal evolution of the PBL thermodynamic structure during the dry and wet seasons in areas away from the direct effects of rain and downdrafts; (2) The observed meridional component of the wind speed has a regular diurnal pattern, with negative values during the night and early morning and positive values during the afternoon. Some seasonal differences are consistent with the idea of a more enhanced river breeze during the dry season, both because of differences in river-land temperature contrast and in the ambient larger-scale boundary wind regime. Areas of negative meridional component (flow toward the river) are confined to layers close to the surface during the dry season in 1985 and occupy a much deeper layer of the flow during the wet season in 1987. The meridional component of the wind shifts trom negative to positive in the dry season in 1985 – an indication of the onset of a river breeze – at Manaus and Ducke Reserve earlier in the day than during the wet season in 1987 at Ducke Reserve, Embrapa and Carapanã. In 1987, the diurnal evolution of the meridional wind component indicates the presence of a much deeper layer with negative

values than in 1985, that also persists longer than in 1985. This seasonal difference is due to the less intense positive meridional circulation during the wet season in 1987; (3) Winds at the surface rotate clockwise describing approximately elliptical trajectories on polar plots. Analysis of the horizontal momentum balance in the lower atmosphere suggests that this rotation occurs because of entrainment of easterly momentum in the morning in concert with the horizontal pressure gradient associated with the river breeze because of the diurnal evolution of the CBL. A simple phase relationship was obtained relating the wind and the forcing showing that the major axes of the local wind ellipse would be perpendicular to the main axis of the horizontal pressure gradient ellipse in the absence of friction. When friction is included, the major axes become parallel; (4) Diurnal rotation of the horizontal temperature and pressure gradients is consistent with the hypothesis of a thermal circulation induced by the thermal contrast between the rivers and the adjacent forest (a "river breeze"). A perturbation high pressure area is located over the area of the river during the day time. During all times of the day the surface pressure and temperature gradients are out of phase. (5) The observed temperature contrast between the Negro River and the adjacent forest in the dry season of 1985 was of the order of 6 K at night and about 3 K during the day. Wind measurements indicate the presence of a circulation that resembles a land breeze during the early morning with convergence over the Negro river area, and a river breeze during the afternoon when the horizontal wind pattern shifts to divergence over the river. (6) Analysis of tethersonde data indicates the existence of two classes of boundary-layer wind maxima, referred to here as J1 and J2. The J1 cases are associated with vertical directional wind shear and occur in a shallow layer (200–400 m). The J2 cases are characterized by no vertical directional shear and are spread over a deeper layer (400–600 m). There were more J1 cases in the dry season (1985) and J2 cases in the wet season (1987). In 1985, the J1 cases are associated with disturbed weather and J2 with undisturbed weather. In 1987, the J1 cases are associated with large systems that appear to propagate from the coast, while the J2 cases are confined to basin and locally occurring systems. The J1 and J2 cases occur on days with more intense radiative cooling in both 1985 and 1987, indicating a relation between LLM and the thermal contrast induced by the river-forest system.

We conclude that the diurnal oscillation in the local wind at the surface can plausibly be explained in terms of the combined effect of an oscillating horizontal pressure gradient force and the vertical distribution of momentum within the PBL, by using a layer-integrated equation of motion. The discrepancies are attributed to the afternoon intensification of subsidence due to cumulus convection.

Acknowledgements

A. P. Oliveira acknowledges support of the Fundacão de Amparo a Pesquisa de São Paulo (FAPESP), Proc. 86/1263–6 during graduate studies at SUNY Albany.

We are grateful to the Brazilian and American members of the ABLE-2 field team. This work was supported by NASA grants NAG-1–692 and NAG-1–583 to the Atmospheric Sciences Research Center (ASRC), SUNY Albany. Continuing efforts after expiration of these grants have been supported by ASRC. We thank M. Garstang and colleagues at the University of Virginia for providing data and suggestions.

References

Betts, A. K.: 1976, 'The Thermodynamic Transformation of the Tropical Subcloud Layer by Precipitation and Downdrafts', *J. Atmos. Sci.* **33**, 1008–1020.

Brock, F. V., Saum, G. H. and Semmer, S. R.: 1986, 'Portable Automated Mesonet II', *J. Atmos. Ocean. Tech.* **3**, 573–582.

Cleveland, W. S. and Terpenning, I. J.: 1982, 'Graphical Methods for Seasonal Adjustment', *J. Am. Stat. Assoc.* **77**, 52–62.

Dickinson, R. E.: 1987, 'Vegetation and Climate Interactions', in R. E. Dickinson (ed.), *The Geophysiology of Amazonia*, pp. 526.

Fitzjarrald, D., Stormwind, Fisch, G. and Cabral, O.: 1988, 'Turbulent Transport Observed Just Above the Amazon Forest', *J. Geophys. Res.* **93**, 1551–1563.

Fitzjarrald, D., Moore, K., Scolar, J. and Cabral, O.: 1989, 'Daytime Turbulent Exchange Between the Amazon Forest and the Atmosphere, *J. Geophys. Res.* **95**, 16825–16838.

Fujita, T. T. and Wakimoto, R. M.: 1982, 'Effects of Miso- and Mesoscale Obstructions on PAM Winds Obtained During Project NIMROD', *J. Appl. Meteorol.* **21**, 840–858.

Garstang, M., Ulanski, S., Greco, S., Scala, J., Swap, R., Fitzjarrald, D., Martin, D., Browell, E., Shipham, M., Harriss, R., Talbot, R. and Connors, V.: 1989, 'The Amazon Boundary Layer Experiment (ABLE 2b): A Meteorological Perspective', *Bull Am. Meteorol. Soc.* **71**, 19–32.

Greco, S., Ulanski, S., Garstang, M. and Houston, S.: 1992, 'Low-Level Nocturnal Maximum Over the Central Amazon Basin', *Boundary-Layer Meteorol.* **58**, 91–115.

Greco, S., Garstang, M., Ulanski, S., Houston, S. and Swap, R.: 1989, 'Local Circulation Over the Central Amazon Basin', *Proceedings of the Third International Conference on Southern Hemisphere Meteorology and Oceanography*, Nov. 13–17, Buenos Aires.

Greco, S., Ulanski, S., Swap, R., Garstang, M., Shipham, M., Andreae, M. O., Harriss, R. C., Talbot, R. and Artaxo, P.: 1989, 'Rainfall and Surface Kinematic Conditions Over the Central Amazonia During ABLE 2b', *J. Geophys. Res.* **95**, 17001–17014.

Harriss, R. C., Wofsy, S. C., Garstang, M., Browell, E. V., Molion, L. C. B., MacNeal, R. J., Hoell, J. M., Bendura, R. J., Beck, S. M., Navarro, R. L., Riley, J. T. and Snell, R. L.: 1988, 'The Amazon Boundary-Layer Experiment (ABLE 2a): Dry Season 1985', *J. Geophys. Res.* **93**, 1351–1360.

Kusuda, M. and Alpert, P.: 1983, 'Anti-Clockwise Rotation of the Wind Hodograph, Part I: Theoretical Study', *J. Atmos. Sci.* **40**, 487–499.

Martin, C. M., Fitzjarrald, D., Garstang, M., Oliveira, A. P., Greco, S. and Browell, E.: 1989, 'Structure and Growth of the Mixing Layer Over the Amazonian Rain Forest', *J. Geophys. Res.* **93**, 1361–1375.

Molion, L. C. B. and Dellarosa, R. L. G.: 1990, 'Pluviometria da Amazonia: são os dados confiaveis? *Climanalise* **5**, 40–42.

Molion, L. C. B.: 1987, 'Micrometeorology of an Amazonian Rain Forest', in R. E. Dickinson (ed.), *The Geophysiology of Amazonia*, pp. 526.

Oliveira, A. P.: 1990, 'The Dynamics of the Planetary Boundary Layer Over the Amazon Rain Forest', Ph.D. dissertation, Department of Atmospheric Sciences, State University of New York, Albany, 296 pp.

Palmén, E. and Newton, C. W.: 1969, *Atmospheric Circulation Systems. Their Structure and Physical Interpretation*, Academic Press, New York, 603 pp.

Pielke, R. A.: 1984, *Mesoscale Meteorological Modeling*, Academic Press, London.

Riehl, H.: 1979, *Climate and Weather in the Tropics*, Academic Press, London, 611 pp.

Scala, J. R., Garstang, M., Tao, W., Pickering, K. E., Thompson, A. M., Simpson, J., Kirchhoff, V. W. J. H., Browell, W. V., Sachse, G. W., Torres, A. L., Gregory, G. L., Rasmussen, R. A. and Khalil, M. A. K.: 1989, 'Cloud Draft Structure and Trace Gas Transport', *J. Geophys. Res.* **95**, 17015–17030.

Shuttleworth, W. J., Gash, J. H. C., Lloyd, C. R. Moore, C. J., Roberts, Marques Filho, A. O., Fish, G., Silva Filho, V. P., Ribeiro, M. N. G., Molion, L. C. B., Nobre, C. A., Sa, L. D. A., Cabral, O. M. R., Patel, S. R. and Moraes, J. C.: 1984, 'Eddy Correlation Measurements of Energy Partition for Amazonian Forest', *Quart. J. Roy. Meteorol. Soc.* **110**, 1143–1162.

Wippermann, F.: 1973, 'Numerical Study on the Effects Controlling the Low-Level Jet', *Beitr. Physik Atmos.* **46**, 137–154.